Lasers in Eng., Vol. 17, pp. 345–360
Reprints available directly from the publisher
Photocopying permitted by license only

Laser Evaporative Heating: Exact Solution or Temperature Rise Due to Step Input Pulse

H. AL-QAHTANI AND B. S. YILBAS*

KFUPM Box 1913, Dhahran 31261, Saudi Arabia

An exact solution for the temperature distribution during evaporative heating of a solid following a laser input pulse has been formulated. The heat transfer equation was made non-dimensional and the closed form solution obtained using the Laplace transformation method. The speed of the receding surface was expressed after assuming an energy balance in the surface region. A numerical solution of the heat transfer equation was necessary so that the temperature predictions obtained from the closed-form solution can be compared. It is found that the temperature rises rapidly in the early heating period because of the energy gain by the substrate material from the irradiated area and only a little energy diffuses from the surface region to the solid bulk during the heating pulse. The numerical predictions of temperature and closed formed solutions are found to be in good agreement.

Keywords: Laser, step input, pulse, temperature, closed-form.

1 INTRODUCTION

High-intensity laser pulses result in a rapid increase in temperature in the irradiated area of the solid material. Once the temperature exceeds the melting and evaporation temperatures of the substrate, a phase change takes place in the irradiated area. In this case, the vapour front expands into the free space whereas the solid surface recedes towards the solid bulk with a progressive number of laser pulses [1]. However, the speed with which the surface recedes can be modelled after assuming energy equilibrium in the surface area. The predictions of the speed of receding are based on the assumption of equilibrium and agree well with the numerical predictions of evaporation [2]. The exact solution for the temperature distribution due to evaporative heating was presented earlier and the closed-form

*Corresponding author: E-mail: bsyilbas@kfupm.edu.sa

solutions were limited to a time dependent exponentially varying pulse [3] or a constant intensity pulse [4]. However, actual laser pulses can be converted to rectangular pulses [5] and in this case the exact solution for the temperature distribution due to laser evaporative heating can not be formulated. Consequently, an investigation of laser evaporative heating and the formulation of the temperature rise during evaporative heating are necessary for practical purposes.

Many research studies were carried out to investigate the laser pulse heating process. Ready [6] introduced a closed-form solution for the temperature rise in a solid. The closed-form solution was limited only to conduction heating and constant intensity pulses. Yilbas [7] introduced a closed-form solution for the temperature rise due to laser evaporation. The solution was applicable only for constant intensity pulses. Blackwell [8] developed an analytical solution for the temperature distribution allowing convection boundary at the surface. His expression was limited to solid phase heating only and was not applicable to evaporative heating. Lu [9] considered a square-shaped temperature distribution induced by a Gaussian-shaped laser beam. His results did not include surface evaporation and also absorption of the laser beam in the vicinity of the surface. Yilbas [3] derived a closed-form solution for the temperature distribution due to laser evaporative heating. The closed-form solution was obtained for a time exponentially varying pulse. However, some laser pulses are rectangular with respect to time [5] and which can be represented in a time-step input pulse. This necessitates re-formulation of the temperature distribution for time-step input laser pulses.

The closed form solution for a temperature distribution due to a laser step input pulse and the evaporative boundary at the surface resembling laser processing of solid surfaces is new. The formulation of such a heating process and the closed-form solution for a temperature rise enables process optimisation and a reduction in experimental cost and time. Consequently, in the present study, laser evaporation heating of solids has been considered and an exact solution for the temperature distribution due to a time-step input pulse has been formulated. A Laplace transformation method was used to obtain the closed-form solution. A numerical method was introduced to compare the closed-form solution for a temperature rise. The heat transfer equation and boundary conditions are made non-dimensional in order to obtain the general solution for the temperature distribution in the substrate.

2 MATHEMATICAL FORMULATION

The Fourier heat transfer equation for a laser heating pulse can be written as

$$\frac{\partial^2 T}{\partial x^2} + \rho C_p V \frac{\partial T}{\partial x} + I_0 \left(1 - r_f\right) P(t) = \rho C_v \frac{\partial T}{\partial t} \tag{1}$$

with the initial condition at time $t = 0 : T(x, 0) = 0$.

The boundary conditions:

Evaporation of the substrate material is taken into account at the free surface.

$$x = 0 : \left.\frac{\partial T}{\partial x}\right|_{x=0} = \frac{\rho V L}{k}.$$

The distance far away from the surface the substrate material is assumed to have the initial temperature, i.e. at infinity:

$$x = \infty : T(\infty, t) = 0.$$

The speed with which the surface recedes can be written as [1]:

$$V = \frac{I_1}{\rho \left(C_p T_s + L\right)} \tag{2}$$

where $I_1 = I_0 \left(1 - r_f\right)$. The time distribution of the laser step input pulse can be written as [10]:

$$P(t) = I_0 \left[1(t) - 1(t - \Delta t)\right] \tag{3}$$

It should be noted that a unit step input pulse of $1(t)$ is a special case of $1(t - \Delta t)|_{\Delta t \to t}$. Figure 1 shows the laser step input pulse and the receding surface. Since, the heat transfer equation is linear, one can consider the half-pulse response and then apply the superposition principle to obtain the complete solution. Therefore, one can write:

$$\frac{\partial^2 T}{\partial x^2} + \frac{V}{\alpha}\frac{\partial T}{\partial x} + \frac{I_1 \delta}{k}(t - \Delta t)e^{-\delta x} = \frac{1}{\alpha}\frac{\partial T}{\partial t} \tag{4}$$

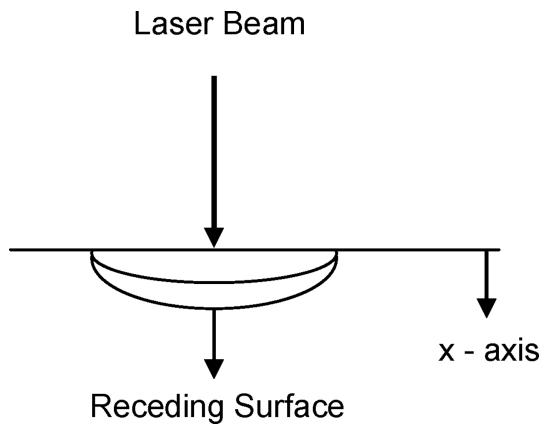

FIGURE 1
Schematic view of pulsed laser heating and the receding surface.

In this case, the initial and boundary conditions are:

$$\begin{aligned} &T(x,0)=0\\ &\tfrac{\partial T}{\partial x}\big|_{x=0}=\tfrac{\rho VL}{k}\delta(t)\\ &T(\infty,t)=0 \end{aligned}$$

Using dimensionless quantities,

$$x^*=\delta x,\ t^*=\alpha\delta^2 t,\ T^*=\frac{k\delta}{I_1}T$$

The governing equations become:

$$\frac{\partial^2 T^*}{\partial x^{*2}}+V\frac{\partial T^*}{\partial x^*}+1\left(t^*-\Delta t^*\right)e^{-x^*}=\frac{\partial T^*}{\partial t^*} \tag{5}$$

with the initial and boundary conditions,

$$T^*\left(x^*,0\right)=0 \tag{6}$$

$$\left.\frac{\partial T^*}{\partial x^*}\right|_{x^*=0}=\beta^*\delta\left(t^*\right) \tag{7}$$

$$T^*\left(\infty,t^*\right)=0 \tag{8}$$

The dimensionless quantities $V^*=V/\alpha\delta$ and $\beta^*=\rho V{}^{L}\!/_{I_1}$ have been introduced.
For convenience, the asterisk (*) will be suppressed.

Taking the Laplace transformation of Eq. (5) with respect to time, one gets

$$\frac{\partial^2\bar{T}}{\partial x^2}+V\frac{\partial\bar{T}}{\partial x}+\frac{e^{-\Delta ts}}{s}e^{-x}=s\bar{T}-T(x,0) \tag{9}$$

$\bar{T}$ is the Laplace transform of the temperature and s is the Laplace variable. Using the initial condition results in:

$$\frac{\partial^2\bar{T}}{\partial x^2}+V\frac{\partial\bar{T}}{\partial x}-s\bar{T}=H_0e^{-x} \tag{10}$$

with the boundary conditions,

$$\left.\frac{\partial\bar{T}}{\partial x}\right|_{x=0}=\beta \tag{11}$$

$$\bar{T}(\infty,s)=0 \tag{12}$$

$$H_0=e^{-\Delta ts}{}/{s}.$$

The last equation is a non-homogeneous ordinary differential equation, which has the solution:

$$\bar{T} = \bar{T}_h + \bar{T}_p$$

T_h and T_p are the homogeneous and particular part of the solution.
To obtain the homogeneous solution, one must find the roots of the characteristic equation:

$$r^2 + Vr - s = 0 \tag{13}$$

The characteristic equation has two roots, namely,

$$r_{1,2} = \frac{-V \mp \sqrt{4s + V^2}}{2}$$

Thus, the homogeneous part can be written as:

$$T_h = C_1 e^{1/2\left(-V-\sqrt{4s+V^2}\right)x} + C_2 e^{1/2\left(V-\sqrt{4s+V^2}\right)x} \tag{14}$$

since the solution is bounded, the second term must vanish:

$$C_2 = 0\,(T(\infty, t) = 0)\,.$$

One can substitute $T = A_0 e^{-x}$ in Eq. (10) to get the particular part of the solution as:

$$\bar{T}_p = \bar{H} e^{-x} \tag{15}$$

where $\bar{H} = \frac{H_0}{1-\upsilon-s}$.
The total solution, which consists of the homogeneous and the particular parts and can be written as:

$$\bar{T}(x, s) = C_1 e^{r_1 x} + \bar{H} e^{-x} \tag{16}$$

The constant C_1 can be determined by applying the boundary condition at the surface, i.e., Eq. (11) to be:

$$C_1 = \frac{\beta + \bar{H}}{r_1} \tag{17}$$

From the above, the temperature solution in the s-domain can be written as:

$$\bar{T}(x, s) = \frac{\beta + \bar{H}}{r_1} e^{r_1 x} + \bar{H} e^{-x} \tag{18}$$

In the unabridged expression, the preceding equation can be rewritten as,

$$\bar{T}(x, s) = \bar{Z}_1(s) + \bar{Z}_2(s) e^{-\Delta t s} + \bar{Z}_3(s) e^{-\Delta t s} \tag{19}$$

where:

$$\bar{Z}_1(s) + \frac{-2\beta}{V + \sqrt{4s + V^2}} e^{\left(-\frac{V}{2} - \frac{1}{2}\sqrt{4s+V^2}\right)x} \tag{20}$$

$$\bar{Z}_2(s) + \frac{-2}{s(1 - V - s)\left(V + \sqrt{4s + V^2}\right)} e^{\left(-\frac{V}{2} - \frac{1}{2}\sqrt{4s+V^2}\right)x} \tag{21}$$

$$\bar{Z}_3(s) + \frac{1}{s(1 - v - s)} e^{-x} \tag{22}$$

The time-space distribution of the temperature $T(x, t)$ can be obtained by applying the inverse Laplace transformation to $\bar{T}(x, s)$ with respect to the variable s. By doing so, one can write the solution in the form:

$$T(x, t) + Z_1(t) + Z_2(t - \Delta t)1(t - \Delta t) + Z_3(t - \Delta t)1(t - \Delta t) \tag{23}$$

Hence, the only remaining task is to find Z_i (t) $(i = 1, 2, 3)$ by applying the inverse Laplace transformation to the corresponding functions $\bar{Z}_i(s)$.

Calculating $Z_1(t)$:

$$\begin{aligned} Z_1(t) &= \mathrm{L}^{-1}\left(\bar{Z}_1(s)\right) \\ &= \frac{1}{2\pi i}\int_{\gamma - i\infty}^{\gamma - i\infty} \bar{Z}_1(s) e^{st} ds \\ &= -2\beta e^{-\frac{V}{2}x} \frac{1}{2\pi i}\int_{\gamma - i\infty}^{\gamma - i\infty} \frac{e^{-\frac{1}{2}\sqrt{4s+V^2}\,x}}{V + \sqrt{4s + V^2}} e^{st} ds \end{aligned}$$

The above expression is not ready to be used according to the standard inversion formula given in [11]. A change of variable $p = V^2 + 4s$ is implemented which yields,

$$Z_1(t) = -\frac{\beta}{2} e^{-\frac{V}{2}x} e^{\frac{-V^2}{4}t} \frac{1}{2\pi i}\int_{\bar{\gamma} - i\infty}^{\bar{\gamma} - i\infty} \frac{e^{\frac{-1}{2}\sqrt{px}}}{V + \sqrt{p}} e^{\frac{p}{4}t} dp \tag{24}$$

$$\bar{\gamma} = V^2 + 4\gamma.$$

Another change of variable is needed in order to put the integration in a suitable form. Let $\sigma = p/4$ which gives $dp = 4d\sigma$ which gives:

$$\begin{aligned} Z_1(t) &= -\beta e^{-\frac{V}{2}x} e^{-\frac{V^2}{4}t} \frac{1}{2\pi i}\int_{\bar{\bar{\gamma}} - i\infty}^{\bar{\bar{\gamma}} - i\infty} \frac{e^{-\sqrt{\sigma x}}}{\frac{V}{2} + \sqrt{\sigma}} d\sigma \\ &= -\beta e^{-\frac{V}{2}x} e^{-\frac{V^2}{4}t} \mathrm{L}^{-1}\left(\frac{e^{-\sqrt{\sigma x}}}{\frac{V}{2} + \sqrt{\sigma}}\right) \end{aligned}$$

$\overline{\overline{\gamma}} = \bar{\gamma}/4$. The term between the two parentheses can be obtained using the rule:

$$\mathrm{L}^{-1}\left(\frac{e^{-m\sqrt{\sigma}}}{n+\sqrt{\sigma}}\right) = \frac{e^{-\frac{m^2}{4t}}}{\sqrt{\pi}\sqrt{t}} - ne^{mn+n^2t}erfc\left(\frac{m}{2\sqrt{t}} + n\sqrt{t}\right) \tag{25}$$

Using the above rule yields:

$$Z_1(t) = -\beta e^{-\frac{V}{2}x} e^{-\frac{v^2}{4t}} \left(\frac{e^{\frac{-x^2}{4t}}}{\sqrt{\pi}\sqrt{t}} - \frac{V}{2}e^{\frac{V^2}{4}t + \frac{V}{2}x} erfc\left(\frac{\sqrt{t}V}{2} + \frac{x}{2\sqrt{t}}\right)\right) \tag{26}$$

Calculating $Z_2(t)$:

$$\begin{aligned} Z_2(t) &= \mathrm{L}^{-1}\left(\overline{Z}_2(s)\right) \\ &= \frac{1}{2\pi i}\int_{\gamma-i\infty}^{\gamma-i\infty} \overline{Z}_2(s)e^{st}ds \\ &= -2e^{-\frac{V}{2}x}\frac{1}{2\pi i}\int_{\gamma-i\infty}^{\gamma-i\infty} \frac{1}{s(1-V-s)(V+\sqrt{4s+V^2})} e^{-\frac{1}{2}\sqrt{4s+V^2}x} e^{st}\, ds \end{aligned}$$

The aforementioned change of variable is used here also. Let $P = V^2 + 4s$, then:

$$Z_2(t) = -\frac{1}{2}e^{-\frac{V}{2}x}e^{\frac{-V^2}{4}t} \frac{1}{2\pi i}\int_{\overline{\gamma}-i\infty}^{\overline{\gamma}-i\infty} \frac{e^{\frac{-1}{2}\sqrt{p}x}}{\left(\frac{p-V^2}{4}\right)\left(1-V-\frac{p-V^2}{4}\right)\left(\upsilon+\sqrt{p}\right)} e^{\frac{p}{4}t}dp$$

The second change of variable $\sigma = p/4$ is then used to get:

$$\begin{aligned} Z_2(t) &= e^{-\frac{V}{2}x}e^{-\frac{V^2}{4}t}\frac{1}{2\pi i}\int_{\overline{\gamma}-i\infty}^{\overline{\gamma}-i\infty} \frac{e^{-\sqrt{\sigma}x}}{\left(\sigma+\xi_1^2\right)\left(\sigma+\xi_2^2\right)\left(\sqrt{\sigma}+\frac{V}{2}\right)}d\sigma \\ &= e^{-\frac{V}{2}x}e^{-\frac{V^2}{4}t}\mathrm{L}^{-1}\left[\frac{e^{-\sqrt{\sigma}x}}{\left(\sigma+\xi_1^2\right)\left(\sigma+\xi_2^2\right)\left(\sqrt{\sigma}+\frac{V}{2}\right)}\right] \end{aligned}$$

where:

$$\overline{\overline{\gamma}} = \bar{\gamma}/4, \xi = -V^2/4, \text{ and } \xi_2^2 = -\frac{V^2}{4} + V - 1.$$

To get an explicit expression of $Z_2(t)$, one needs to find the inverse transformation of the term inside the two brackets as follows:

$$\mathbf{L}^{-1}\left[\frac{e^{-\sqrt{\sigma}x}}{\left(\sigma+\xi_1^2\right)\left(\sigma+\xi_2^2\right)\left(\sqrt{\sigma}+\frac{V}{2}\right)}\right]$$
$$=\mathbf{L}^{-1}\left[\frac{e^{-\sqrt{\sigma}x}}{\left(\sqrt{\sigma}+\xi_1\right)\left(\sqrt{\sigma}+\xi_1\right)\left(\sqrt{\sigma}+\xi_2\right)\left(\sqrt{\sigma}+\xi_2\right)\left(\sqrt{\sigma}+\frac{V}{2}\right)}\right]$$
$$=\mathbf{L}^{-1}\left[\left(\frac{l_1}{\sqrt{\sigma}+\xi_1}+\frac{l_2}{\sqrt{\sigma}+\xi_1}+\frac{l_3}{\sqrt{\sigma}+\xi_2}+\frac{l_4}{\sqrt{\sigma}+\xi_2}+\frac{l_5}{\left(\sqrt{\sigma}+\frac{V}{2}\right)}\right)e^{-\sqrt{x}}\right]$$

where the residues l_i are given in the appendix. The formula given by Eq. (28) is used to invert each term in the preceding expression. Thus,

$$\begin{aligned}
Z_2(t) &= e^{-\frac{V}{2}x}e^{-\frac{V}{4}t}\left[l_1\left(\frac{e^{\frac{-x^2}{4t}}}{\sqrt{\pi}\sqrt{t}}-\xi_1 e^{x\xi_1+t\xi_1^2}erfc\left(\frac{x}{2\sqrt{t}}+\sqrt{t}\xi_1\right)\right)\right]\\
&+l_2\left(\frac{e^{\frac{-x^2}{4t}}}{\sqrt{\pi}\sqrt{t}}-\xi_1 e^{-(x\xi_1)+t\xi_1^2}erfc\left(\frac{x}{2\sqrt{t}}+\sqrt{t}\xi_1\right)\right)\\
&+l_3\left(\frac{e^{\frac{-x^2}{4t}}}{\sqrt{\pi}\sqrt{t}}-\xi_2 e^{x\xi_2+t\xi_2^2}erfc\left(\frac{x}{2\sqrt{t}}+\sqrt{t}\xi_2\right)\right)\\
&+l_4\left(\frac{e^{\frac{-x^2}{4t}}}{\sqrt{\pi}\sqrt{t}}-\xi_2 e^{-(x\xi_2)+t\xi_2^2}erfc\left(\frac{x}{2\sqrt{t}}+\sqrt{t}\xi_2\right)\right)\\
&+l_5\left(\frac{e^{\frac{-x^2}{4t}}}{\sqrt{\pi}\sqrt{t}}-\frac{V}{2}e^{x\frac{V}{2}}+t\frac{v^2}{2}erfc\left(\frac{x}{2\sqrt{t}}+\sqrt{t}\frac{V}{2}\right)\right)
\end{aligned} \tag{27}$$

Calculating $Z_3(t)$:

$$\begin{aligned}
Z_3(t) =& \mathrm{L}^{-1}\left(\frac{-e^{-x}}{s(s+V-1)}\right)\\
=& \frac{1-e^{t(1+V)}}{1+V}e^{-x}
\end{aligned} \tag{28}$$

Hence since the functions $Z_1(t)$, $Z_2(t)$, and$Z_3(t)$ have been obtained, the temperature distribution is known explicitly (Eq. (23)). Mathematical

TABLE 1
Material properties and the laser pulse parameters used in the simulations.

ρ Kg/m^3	δ 1/m	L J/kg	Cp J/kgK	k W/mK	T (K)	Io (W/m^2)	Δt
7880	6.16×10^6	6258153.8	460	80.3	3030	10^{13}	2, 4, 10

software was used to compute the temperature distribution. Parameters used in the computation are given in Table 1. A numerical method using finite difference is used to predict the numerical temperature rise.

3 RESULTS AND DICUSSIONS

An analytical solution to describe laser evaporation following a step-input pulse was considered and an exact solution for the temperature distribution has been obtained. Since the heat transfer equation and the boundary conditions were made non-dimensional, the closed-form solution can be applied to all materials. The closed-form solution of the temperature distribution has been compared with numerical solutions. Table 1 gives the laser pulse parameters used in the closed-form and in numerical solutions.

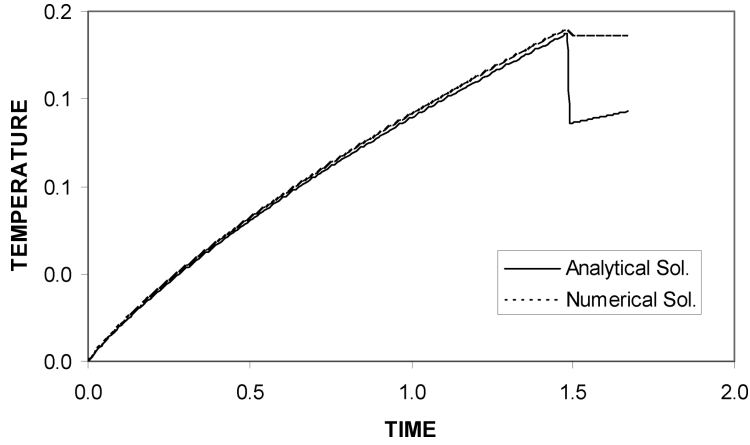

FIGURE 2
Comparison of the temporal variation of dimensional surface temperature as obtained from the closed form and numerical solutions for $\Delta t = 5$.

Figure 2 shows the variation of the surface temperature with time obtained from the numerical predictions and the closed-form solution. It can be observed that both results are in good agreement. However, once the evaporation temperature is reached, the temperature in the closed form solution decreases whereas it remains at the evaporation temperature for the numerical solution. This is due to the mushy zone considered in the numerical

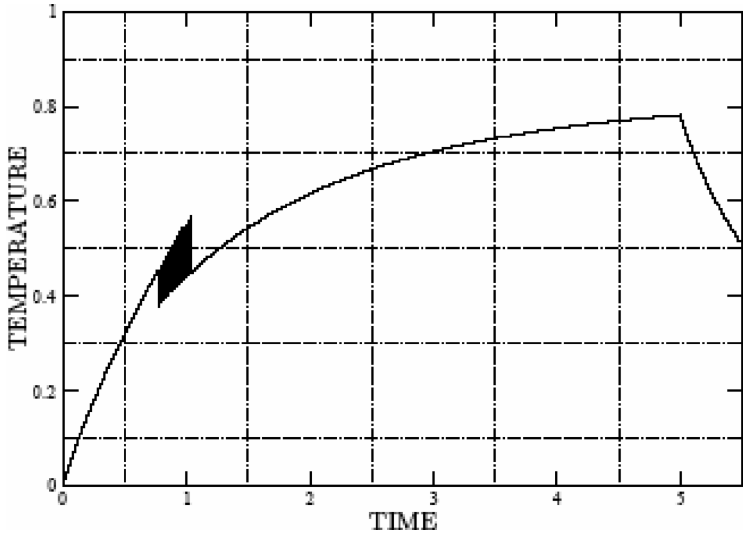

FIGURE 3
Temporal distribution of dimensionless temperature at x = 0 for $\Delta t = 5$.

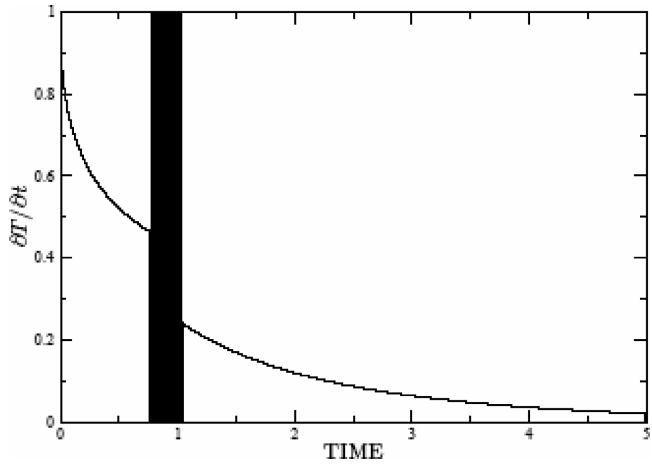

FIGURE 4
Temporal distribution of the time-derivative of temperature at x = 0 for $\Delta t = 5$.

solution. Figure 3 shows the variation of the surface temperature with time while Figure 4 shows the time derivative of the surface temperature. The rise in surface temperature is high in the early heating period ($t \leq 0.1$) but as time progresses the rate of the temperature rise is reduced. This is due to the gain in the internal energy of the substrate in the surface region. In

the early heating period, the internal energy gain from the irradiated field is high and the conduction loss from the surface to the solid bulk material is small because of the low temperature gradient. As time progresses, the temperature gradient in the surface area is high, which in turn increases the diffusion of heat from the surface region to the substrate. Consequently, the internal energy gain has been retarded by diffusion in the surface, thus lowering the surface temperature. With time, the evaporation temperature of the substrate is reached. The temperature is reduced sharply due to the latent heat of evaporation. The internal energy is reduced by an amount equal to the latent heat of evaporation in the surface. This results in a sharp decay in the surface temperature. This situation repeats itself at about the evaporation temperature until the temperature is greater than that of evaporation. A similar situation can be seen in the numerical predictions, provided that the temperature remains at the evaporation temperature in the mushy zone [2]. As the time is increased beyond the evaporation time, the temperature rises continuously until the laser pulses stop. Moreover, the rate of temperature increase beyond the evaporation temperature is less than that of below the evaporation temperature. This situation can be seen in Figure 4., in which case, $\partial T / \partial t$ is small beyond the evaporation temperature. The slow rise in surface temperature is attributed to one or all of the following: (i) some fraction of the energy gained from the irradiated field is dissipated during the evaporation process and (ii) the energy dissipation by diffusion from the surface to the bulk material due to attainment of a higher temperature gradient in the later heating period. Once the laser pulse has been stopped the cooling cycle starts and the internal energy gain from the irradiated field ceases. Consequently, diffusion of energy, from the surface region to the solid bulk, reduces the temperature at the surface rapidly. However, the variation of temperature with time at different depths below the surface is different, particularly at the time of temperature settling (time corresponding to temperature oscillations during initial evaporation) during which the evaporation process increases as the depth below the surface increases. This is due to the amount of irradiated energy absorbed by the substrate material at some depth below the surface, i.e., the absorbed energy decreases with increasing depth (Lambert's law). Thus, the energy balance between the internal energy gain from the irradiated field and the energy loss by diffusion from the surface to the bulk modifies causes the temperature change with time to vary on the surface.

Figure 5 shows temperature distribution inside the substrate material at various heating periods. Since evaporation takes place on the surface and the amount the surface recedes towards the solid bulk is small during the early heating period, temperature settlement is not shown in the figure. Consequently, temperature profiles start just below the surface in the figure due to the shallow evaporation depth. The temperature decays gradually

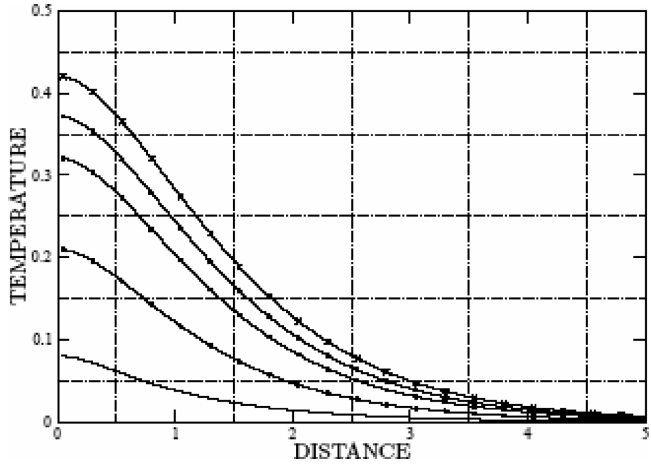

FIGURE 5
Spatial distribution of temperature inside the substrate material for $\Delta t = 5$.

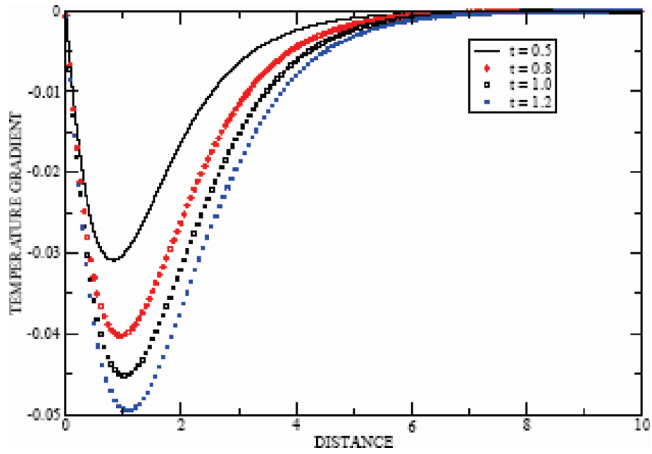

FIGURE 6
Spatial distribution of the temperature gradient inside the substrate material for $\Delta t = 5$.

in the surface region and as the distance below the surface increases the temperature decay is marked. This can be seen in Figure 6. in which the temperature gradient is shown. The temperature gradient at the surface is not zero because of the evaporation boundary on the surface. Moreover, since the distance to the surface increases, the temperature decays gradually. This is because of the energy transfer mechanism in the substrate material. In the region limited by the absorption depth, the energy gain from the irradiated

field is high. The temperature rises in this region and an energy transfer by diffusion from this region to the solid bulk is insignificant compared to the energy gain in the surface. As the depth below the surface increases beyond the absorption depth, energy transfer by diffusion dominates the energy transport process. In this case, higher temperature gradients result in a higher energy transfer to the bulk material by diffusion. The energy balance between the internal energy gain from the irradiated field and the energy transfer by diffusion from the surface region to the solid bulk reaches equilibrium at the point of the maximum temperature gradient. The internal energy gain is important for depths extending from the surface to the site of the maximum temperature gradient and the energy transfer by diffusion is important at a depth between the site of maximum temperature gradient and the bulk material.

4 CONCLUSIONS

Laser evaporative heating following step-input pulses have been considered. The laser pulses can be made to resemble rectangular pulses (step-input pulses). In this case, the exact solution obtained previously for temperature distributions due to exponential pulses is not valid for laser step-input pulse heating. Thus, an exact solution for the temperature distribution for step-input pulses is interesting, as an effort must be made to reduce the time of numerical calculations. An exact solution for the temperature distribution can be obtained by solving the heat transfer equation via using the Laplace transformation method. The evaporation of the surface is modelled after consideration of the energy balance in the surface region. This provides for the surface receding during the evaporation process. Since the latent heat of evaporation is significantly higher than the latent heat of fusion and the laser output intensity is high, evaporation is considered to be the governing mechanism in the analysis. It is found that the numerical prediction of the temperature distribution agreed well with the results of the exact solution. The temperature rises faster in the early heating period because of the internal energy gain from the irradiated region and a small energy dissipation by diffusion from the surface to the solid material. Once the evaporation temperature has been reached, temperature fluctuations occur due to the latent heat of evaporation. The energy gain from the irradiated field is comparable to the latent heat of evaporation at the surface. This situation continues until the temperature is higher than the evaporation temperature. The temperature settlement time is small and increases as the depth below the surface increases. Moreover, as the temperature increases beyond the evaporation temperature, the temperature rises steadily until pulsing is stopped, when cooling starts. In the cooling period, the temperature falls rapidly due to the internal energy gain from the irradiated field does not

take place and diffusion becomes the sole mechanism in the substrate The maximum temperature gradient occurs at some distance below the surface and the energy balance between the internal energy gain and the energy transfer by diffusion is attained at this location.

ACKNOWLEDGMENTS

The authors acknowledge the support of King Fahd University of Petroleum and Minerals, Dhahran, Saudi Arabia for this work.

NOMENCLATURE

Cp	Specific heat capacity (J/kgK)
I_1	Power intensity ($I_o(1-r_f)$) (W/m^2)
Io	Power intensity (W/m^2)
k	Thermal conductivity (W/mK)
L	Latent heat of evaporation (J/kg)
s	Laplace variable
P(t)	Temporal variation of laser pulse intensity
r_f	Reflection coefficient
T(x,t)	Temperature (K)
T*(x*,t*)	Dimensionless temperature (= $T(x,t)\frac{k\delta}{I_1}$)
t	Time (s)
Δt	Pulse length of the laser pulse (s)
V	Receding speed (m/s)
V*	Dimensionless recession velocity (=$\frac{V}{\alpha\delta}$)
x	Distance (m)
x*	Dimensionless distance (=$x\delta$)
α	Thermal diffusivity (m^2/s)
$\beta*$	$= \frac{\rho V L}{I_1}$
δ	Absorption coefficient (1/m)
ρ	Density (kg/m^3)

REFERENCES

[1] Yilbas, B. S., Sahin, A. and Davies, R. (1995). "Laser heating mechanism including evaporation process initiating the laser drilling", Int. Journal, Mach. Tools and Manufact. Vol.*35*, No.7, pp.1047–1062.

[2] Mansour, S. B. and Yilbas, B. S. (2006). "Laser pulse heating of steel surface: consideration of phase change process", Numerical Heat Transfer, Part A, Vol. *50*, No. 8, pp. 787–807.

[3] Yilbas, B. S. (2002). "A closed form solution for temperature rise inside solid substrate due to time exponentially varying pulse", Int. J. Heat Mass Transfer, Vol.*45*, pp. 1993–2000.

[4] Yilbas, B. S. and Sahin, A. Z. (1994). "Laser heating mechanism including evaporation process", Int. Comm. in Heat and Mass Transfer , Vol. *21*, No.4, pp.509–518.

[5] Amada United Kingdom Limited, Spennells Valley Road, Kidderminster, Worcestershire DY10 1XS, U.K.

[6] Ready, J. F. (1963). "Effects due to absorption of laser radiation", J. Appl. Phys., Vol.*36*, pp. 462–470.

[7] Yilbas, B. S. and Shuja, S. Z. (2003). "Laser non-conduction limited heating and prediction of surface recession velocity in relation to drilling", Proc Instn Mech Engrs, Part C: J. Mechanical Engineering Science, Vol. *217*, pp.1067–1076.

[8] Blackwell, B. F. (1990). "Temperature profile in semi-infinite body with exponential source and convective boundary conditions", ASME, J. Heat Transfer, Vol.*112*, pp.567–571.

[9] Lu, Y. (1994). "Square-shaped temperature distribution induced by a Gaussian-shaped laser beam", Appl. Surf. Science, Vol. *81*, pp. 357–364.

[10] Yilbas, B. S. and Kalyon, M. (2006). "Repetitive laser pulse heating analysis: pulse parameter variation effects on closed form solution", Applied Surface Science, Vol. *252*, pp. 2242–2250.

[11] Abramowitz, M. and Stegun, I. A. (1965). "Handbook of Mathematical Functions", Dover, New York.

APPENDIX

$$
\begin{aligned}
l_1 &= \frac{1}{2\xi_1(\xi_1^2-\xi_2^2)(\xi_1+\xi_3)} \\
l_2 &= \frac{1}{2\xi_1(\xi_1^2-\xi_2^2)(\xi_1-\xi_3)} \\
l_3 &= \frac{1}{2\xi_2(\xi_1^2-\xi_2^2)(\xi_1+\xi_3)} \\
l_4 &= \frac{1}{2\xi_2(\xi_2^2-\xi_1^2)(\xi_2-\xi_3)} \\
l_5 &= \frac{1}{(\xi_1^2-\xi_3^2)(\xi_2^2-\xi_3^2)}
\end{aligned}
$$

where $\xi_1^2 = -V^2/4, \quad : \xi_2^2 = -\frac{V^2}{4} + V - 1$ and $\xi_3 = -V/2$